MR in Cystic Tumors of the Pancreas

5

Riccardo Manfredi, Sara Mehrabi,
Enrico Boninsegna, and Roberto Pozzi Mucelli

5.1 Introduction

Cystic neoplasms of the pancreas are rare tumors that arise from elements of the epithelial component of the pancreas. They represent 1 % of all pancreatic cancers and 10 % of all cystic lesions of the gland [1]. Nowadays cystic neoplasms of the pancreas are diagnosed more frequently due to the spread of increasingly accurate imaging techniques. The diagnosis is often incidental because they tend to be asymptomatic or they present nonspecific symptoms.

Although they are considered benign lesions in the early stages, progressive malignant degeneration is possible for the occurrence of dysplastic foci [2].

The WHO classification is based to the histological features of the wall with special reference to the epithelium lining, the main element in the differential diagnosis with nonneoplastic cystic lesions of the pancreas [3]. This classification distinguishes serous cystic neoplasms (SCNs), mucinous cystic neoplasms (MCNs), intraductal papillary mucinous neoplasms (IPMNs), and solid pseudopapillary neoplasms (SPNs).

R. Manfredi, MD, MBA (✉) • S. Mehrabi, MD
E. Boninsegna, MD • R. Pozzi Mucelli, MD
Department of Radiology, Policlinico G. B. Rossi, University of Verona, Verona, Italy
e-mail: riccardo.manfredi@univr.it; saraprinaz@yahoo.it; boninsegnae@gmail.com; roberto.pozzimucelli@univr.it

A correct classification is particularly important because it affects the subsequent choice of therapy that it is not necessarily surgery. Those with a greater potential for malignant transformation are MCNs, IPMNs of the main pancreatic duct, and SPNs, which require a surgical resection, while SCNs and branch-duct IPMNs have a very low malignant potential and can be managed with a radiological follow-up [4].

Pancreatic neuroendocrine tumors (NETs) present as cystic lesions in approximately 5 % of cases, with radiological features similar to other cystic lesions of the pancreas. Their appearance can be identical to SCNs, MCN, or SPNs, and often a definitive diagnosis can be obtained only after histological examination.

Magnetic resonance imaging (MRI) is the most important technique in the evaluation of cystic neoplasms of the pancreas, because it allows to analyze the morphology of the lesions, their content, and the relationship with the pancreatic ductal system [5].

With regard to other imaging methods, ultrasonography can in many cases identify a cystic lesion of the pancreas, but it does not have the same spatial and contrast resolution of MRI, it is affected by patient's constitutional factors, and not least it depends from the operator experience [5].

Although the endoscopic ultrasonography may help to overcome some of these limitations, it remains an invasive technique. CT can better depict the presence of calcification, but it does not allow to identify the typical features which

M. Del Chiaro et al. (eds.), *Cystic Tumors of the Pancreas*, DOI 10.1007/978-3-319-31882-0_5

are often essential for the differential diagnosis of these neoplasms [5].

In the following part of the text, the various pancreatic cystic neoplasms will be described, with particular attention to the MRI aspects useful for the differential diagnosis.

5.2 Serous Cystic Neoplasms

5.2.1 Background

Serous cystic neoplasms (SCNs) are divided according to the WHO classification in serous cystadenoma and serous cystadenocarcinoma, although the second was reported in the literature in a very limited number of cases.

SCNs are more frequent in female patients (male/female, 1:3), with an average age of 62 years (range 35–84 years). They can be found in any pancreatic region, but they are more frequent in the head (>50 %). The size can be extremely variable, from 1–2 cm to 20–25 cm (average 6–10 cm) [6].

To date the only established association between SCNs and others neoplasm is von Hippel-Lindau disease, an autosomal dominant condition caused by mutations of suppressor gene VHL.

More than 50 % of serous cystadenomas are asymptomatic and discovered incidentally during diagnostic evaluations conducted for other symptoms (often unrelated). Symptoms are nonspecific: abdominal pain (25 %), anorexia and dyspepsia (10 %), rarely jaundice (7 %), weight loss, and a palpable abdominal mass. Clinical symptoms are commonly seen in serous cystic neoplasms larger than 4 cm [7]. Symptoms are related to a mass-compressing effect and are nonspecific. Even when present, symptoms often do not raise immediate alarm, so it is not uncommon that the onset of symptoms may precede the diagnosis of a few years (average a year and a half). The most common symptom is abdominal pain, but only 35 % of patients who present with symptomatic serous cystadenoma present a typical pancreatic pain ("bar" irradiation).

With regard to laboratory tests, there are no tumor markers or tests indicative of the biological behavior of the lesions [8].

5.2.2 Pathology

Serous cystadenoma frequently appears as a rounded, full of liquid fluid, and transparent cystic mass, with lobulated and well-defined margins. Dimensions may vary in diameter from 1 to 25 cm (average 6–11 cm). They are usually single lesions, but, especially in the von Hippel-Lindau patients, multiple lesions or multifocal and confluent neoplasms can be present. There is no communication between the lesion and the main pancreatic duct. Macroscopically they are divided according to the number and size of cysts into three subtypes: microcystic, macrocystic, and mixed type [1, 6].

In the classical form, microcystic lesions present well-circumscribed lobulated margins. When spongy texture is present, it is formed by multiple (>6) small cysts that vary from 1 to 5 mm in diameter. The cysts are filled with serous transparent fluid. In 30 % of cases, there is a typical central "star-shaped" scar composed of white nodules and fibrosis. The scar often has calcium deposits, which may appear to radiological investigations as starry or punctuated calcifications.

In the macrocystic form, the lesion is characterized by the presence of a small number (<6) of larger cysts. The intracystic fluid can be clear and transparent or a brownish fluid with blood. The cutting surface shows the presence of a quantifiable number of cysts or, sometimes, a single cyst (unilocular variant), with a diameter between 2 and 15 cm. This form typically does not present the central scar [3, 6].

In mixed form, the lesion is characterized by the presence of larger cysts, situated on the periphery of the lesion, and microcysts in the center. There may be a central scar.

Microscopically the different forms of cystadenoma are indistinguishable and show the typical serous epithelium that can vary from cubical to squamous, in which the cells present clear cytoplasm and round nuclei. Cytological atypia and

mitotic activity are rare. Typically in these tumors glycogen is intracellular (positive for periodic acid-Schiff) and intracellular mucin is absent. The neoplastic stroma is highly vascularized. The walls that separate the cysts are larger and contain hemosiderin-laden macrophages and sometimes islets of Langerhans and trapped exocrine acini. The fibrous scar characteristic of microcystic variant is also formed by hyalinized tissue, frequently associated with calcification. All variants of serous cystadenoma lack a fibrous pseudocapsule.

Malignant serous cystic neoplasms are rare. Cystic adenocarcinomas are associated with lymphovascular and perineural invasion, extension to adjacent organs, and detection of metastatic disease in the regional lymph nodes and liver. A minimal nuclear atypia and a more prominent papillary architecture have been described in some serous cystadenomas presenting also a positivity for the proliferation marker Ki-67 and an overexpression of the p53 protein. These features are considered premalignant and are associated with a risk of malignant transformation of 3 % [2, 6].

5.2.3 MRI

Magnetic resonance imaging (MRI) plays an important role in the characterization of cystic tumors: the multiplicity of sequences on the various planes of the space and the use of the contrast medium allow to obtain information on the morphology and composition of the lesion. In addition, the use of magnetic resonance cholangiopancreatography (MRCP) allows a better assessment of the relationship between the cystic mass and the main pancreatic duct, helpful in the differential diagnosis between serous cystadenoma and branch-duct intraductal papillary mucinous neoplasm [5].

Microcystic serous cystadenoma (Figs. 5.1 and 5.2) appears hypointense on T1-weighted images in respect to the adjacent parenchyma, with homogeneous signal intensity in the lesion; septa and calcifications are not well visible. Rarely hemorrhagic foci within the mass can be identified. On T2-weighted images, it appears as a group of small cysts, with hyperintense fluid content, without any communication with the main pancreatic duct, separated each other by thin fibrous septa. It can present a pathognomonic central fibrous scar. On T1-weighted images after contrast administration, the information obtained are essentially comparable to those obtainable by computed tomography (CT): contrast enhancement of walls and septa in the arterial phase, allowing optimal visualization of the "honeycomb" structure, which is even better recognizable in the portal venous phase.

T2-weighted images are important to evaluate the content of the cystic lesion (fluid, presence of septa) and pancreatic ductal system. The use of images with fat saturation allows to suppress the high intensity of the signal from the adipose tissue and consequently to increase the representation of the internal structure of the lesion. MRCP sequences give an optimal representation of the pancreatic ductal system. T1-weighted fat saturated images can identify foci of internal bleeding or protein deposits, features more often seen in pseudocysts or degenerated solid tumors of the pancreas. In addition, T1-weighted images are useful for evaluating the adjacent pancreatic parenchyma to identify, for example, signal changes suggestive of chronic pancreatitis, especially in those cases where a pseudocyst is part of the differential diagnosis [3, 5].

Diffusion-weighted imaging (DWI) is nowadays very important in the diagnosis of pancreatic masses. In serous cystadenomas, the values of apparent diffusion coefficient (ADC) are substantially similar to those of simple cysts: in b1000 sequences, the lesion appears hypointense, not presenting signal restriction in ADC. For this reason, information obtained from diffusion images do not allow an adequate differential diagnosis of serous cystadenoma from mucinous cystic neoplasms [9].

The presence of a mass with a spongy appearance and central calcifications in the pancreatic head in a woman is diagnostic for serous cystic neoplasm, especially when the remaining pancreatic parenchyma is normal, without dilation of the Wirsung duct. In this case, you need no other

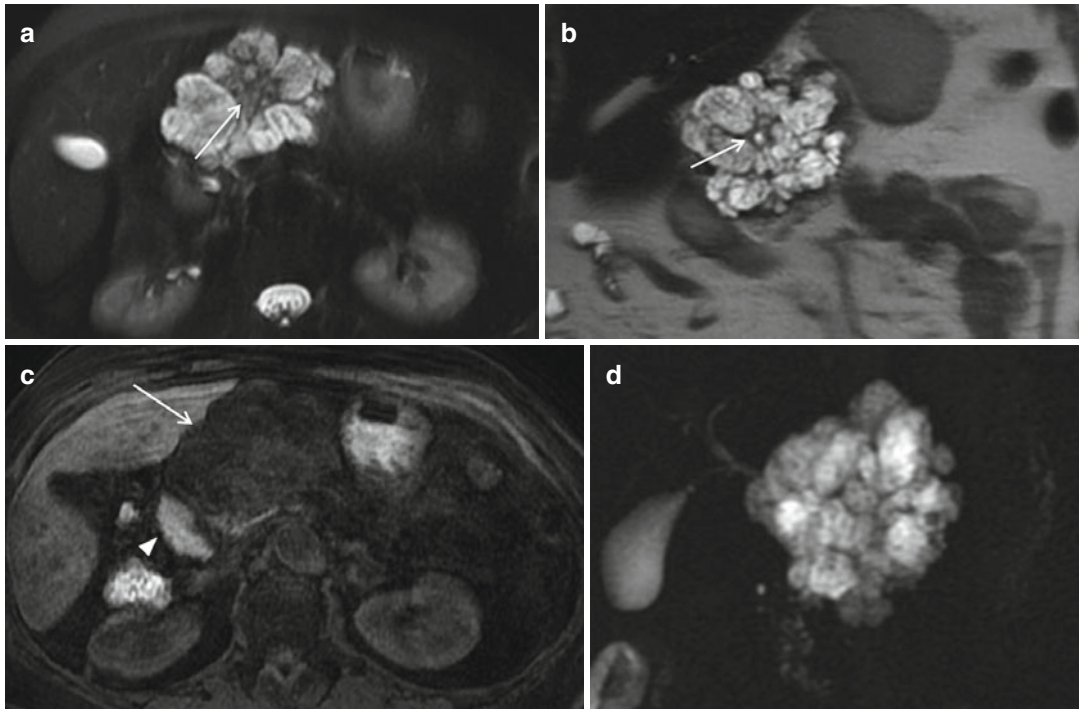

Fig. 5.1 A 69-year-old female patient with serous cystadenoma in the pancreatic head. (**a**, **b**) Axial (**a**) and coronal (**b**) T2-weighted images: the lesion presents multiple hyperintense microcysts, with septa that radiate from the central scar (*arrow*). (**c**) Axial T1-weighted GRE image with fat saturation: the content of the lesion (*arrow*) is homogeneously hypointense compared to the adjacent pancreatic parenchyma (*arrow head*). (**d**) MRCP image: the cystic lesion is well visible; main pancreatic duct cannot be depicted

diagnostic investigations, because the choice of treatment is made on the basis of clinical presentation and the patient's general condition.

Serous cystadenoma is in the differential diagnosis of intraductal papillary mucinous neoplasms (IPMNs), and it is essential to detect a possible communication with the main pancreatic duct, never present in serous cystadenoma.

The diagnosis can also be considered definitive when the lesion shows a mixed micro-macrocystic aspect, with cysts >2 cm at the periphery of the lesion and the microcysts in center.

The most difficult diagnosis is a lesion with oligocystic-macrocystic pattern (number of cysts <6, cyst diameter >2 cm): this variant is very similar to mucinous cystic neoplasms. The presence of papillary projections or mural nodules in the cysts is suspicious for borderline mucinous cystadenoma or mucinous cystadenocarcinoma. These nodules appear as areas of low signal intensity in T2-weighted images and present contrast enhancement.

In the presence of unilocular cystic lesions, the differential diagnosis is with pseudocyst; other possibilities are intraductal papillary mucinous neoplasms and lymphoepithelial cysts. These lesions can be differentiated from pseudocysts because of the lack of clinical, laboratory, and imaging findings (pancreatic inflammation, atrophy or parenchymal calcifications, duct dilation, or intraductal stones) suggestive of pancreatitis [10]. Pseudocysts are also more common in the body-tail of the pancreas and appear hypointense on T1-weighted images and hyperintense (if filled with fluid) or mixed intensity (if filled with fluid and debris) on T2-weighted images. At MRCP pseudocysts appear hyperintense and contiguous to the main pancreatic duct.

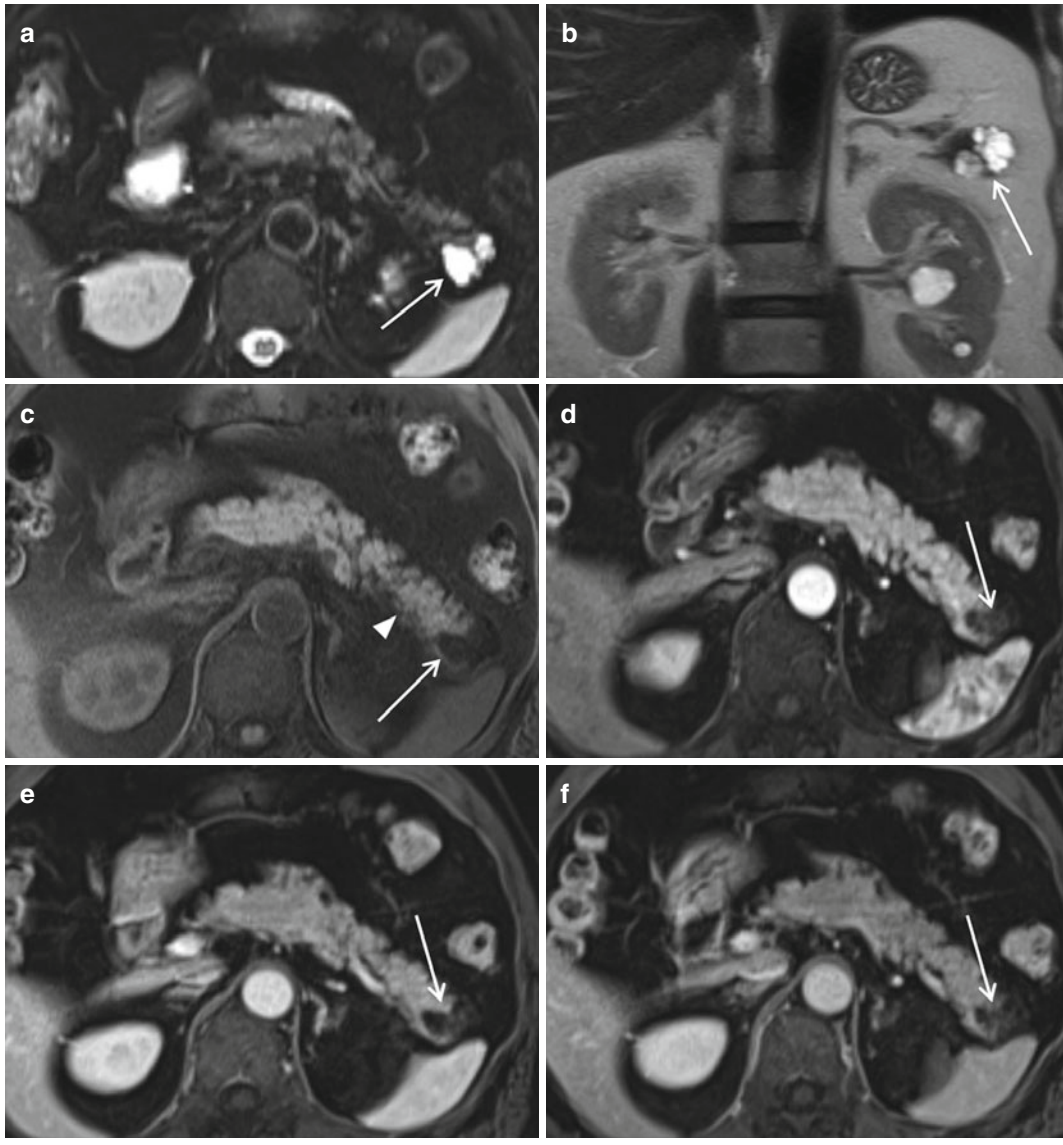

Fig. 5.2 A 56-year-old male patient with serous cystadenoma in the pancreatic tail. (**a**, **b**) Axial (**a**) and coronal (**b**) T2-weighted images: the lesion presents multiple hyperintense microcysts with septa (*arrow*). (**c**) Axial T1-weighted GRE image with fat saturation: the content of the lesion (*arrow*) is homogeneously hypointense compared to the adjacent pancreatic parenchyma (*arrow head*). (**d**–**f**) Axial T1-weighted GRE images with fat saturation after contrast administration, in pancreatic (**d**), portal (**e**), and late (**f**) phases: a progressive contrast enhancement of septa (*arrow*) is visible

When the differentiation is not possible with diagnostic imaging, symptomatic patients should undergo surgery. Asymptomatic patients with unilocular cyst with thin walls, especially if small, can be monitored over time with CT or MRI [7].

Note, in most cases, serous cystadenoma is presented as a single lesion, except in von Hippel-Lindau patients. In this syndrome, the pancreas is involved in 15–30 % of cases with the presence of multiple serous cystadenomas, without a preferential localization. The average age at diagnosis is 30 in these cases. The diagnosis of von Hippel-Lindau must therefore always be considered when multiple pancreatic cysts are

found in an asymptomatic patient without clinical evidence of pancreatitis. In these cases, a complete clinical and radiological evaluation should also include the central nervous system (most common manifestation: cerebellar hemangiomas), eye (retinal hemangiomas), kidneys (cysts, clear cell carcinoma), and adrenal glands (pheochromocytoma).

5.3 Mucinous Cystic Neoplasms

5.3.1 Background

Mucinous cystic neoplasms (MCNs) are rare cystic lesion of the pancreas [2, 5], representing approximately 2–5 % of all exocrine pancreatic tumors and 17 % of cystic neoplasms of the pancreas [11]. They occur almost exclusively in women between the third and eighth decade, with peak incidence in the fifth decade (average age 49). The majority of lesions occur in the body-tail of the pancreas, while the head is only rarely involved.

In recent years, some evidences have suggested the possible origin of MCNs by ectopic primordial ovarian tissue that undergoes malignant degeneration [12].

The possible derivation of the stromal component of MCNs from ovarian primordial gonad is supported by their morphology and the positive immunohistochemical analysis for inhibin, estrogen, and progesterone receptors, indicating precisely stromal luteinization.

In addition, the embryological origin of the pancreas reinforces this hypothesis. The dorsal pancreatic bud, which gives rise to the body and tail of the pancreas and a small part of the pancreatic head, and the left primordial gonad are very close in an early stage of development (fourth to fifth week), unlike the ventral pancreatic bud, which gives rise to most of the pancreatic head, which is separated from the primordial right gonad from the hepatobiliary gem. This makes it plausible that the primordial egg cells could easily be incorporated in the pancreas and would also explain the predilection of MCNs for the body-tail of the pancreas [12].

The clinical presentation depends on the size of the tumor: small tumors are asymptomatic and discovered incidentally; larger tumors produce symptoms by compression of adjacent structures and palpable abdominal mass.

MCNs constitute a category of potentially malignant cystic neoplasms of the pancreas: benign forms such as mucinous cystadenomas (MCAs) are known precursors of invasive forms such as mucinous cystoadenocarcinomas (MCACs) [2, 3].

Consequently, it is crucial to plan a proper diagnostic and therapeutic strategy to differentiate MCNs from other pancreatic cystic tumors with a benign biological behavior addressed to follow-up, such as serous cystadenomas (SCAs) and other cystic lesions of the pancreas, such as pseudocysts and nonneoplastic mucinous cysts.

In addition, MCNs enter into the differential diagnosis with another category of cystic tumors which also have malignant potential such as intraductal papillary mucinous neoplasm (IPMNs) [13].

5.3.2 Pathology

Mucinous cystic neoplasms (MCNs) are characterized by the presence of mucin-secreting epithelial cells, supported by ovarian-type stroma, which delimits a cystic cavity without communication with the pancreatic ductal system [2].

The presence of mucin-secreting columnar epithelium distinguishes MCNs from serous cystadenoma, solid pseudopapillary neoplasm, and cystic neuroendocrine tumor.

The absence of communication with the pancreatic ductal system is fundamental in the distinction between MCNs and IPMNs. In fact, even IPMNs are characterized by the presence of mucin-secreting epithelial cells, and this has led in the past some pathologists to interpret MCNs and IPMNs as a single entity.

According to the degree of epithelial dysplasia, they can be classified into adenoma, borderline tumor, and carcinoma, invasive or noninvasive, although all MCNs of the pancreas should be considered potentially malignant [2].

The progression from cystadenoma to cystadenocarcinoma is also suggested by the average age of onset of two forms: the average age of onset of cystoadenocarcinomas is 54.2 years, while the average age of onset of borderline forms or adenomas is 44.7 years.

MCNs appear as round masses with smooth surface and fibrous pseudocapsule of variable thickness, with frequent calcifications. Tumor size can vary widely in a range between 2 and 35 cm, average between 6 and 10 cm.

MCNs usually are macrocystic and multilocular, rarely unilocular, with cystic spaces ranging from a few to several centimeters in diameter, containing mucin or mucin dense mixed hemorrhagic-necrotic material. The inner surface of unilocular tumors usually appears smooth and shiny, while tumors often show multilocular papillary projections and nodules.

The malignancy of MCNs correlates significantly with the presence of papillary projections and/or nodules.

There is no communication between the tumor and the main pancreatic duct.

MCNs show two distinct components: an inner layer and an outer layer with epithelial cells very similar to ovarian stroma. The epithelium often shows areas with pseudopyloric, gastric, small bowel, and colon differentiation, while ovarian stroma is composed of densely packed cells with round nuclei. About half of the tumors also contain endocrine cells at the base of the columnar cells. The spectrum of cell differentiation varies from columnar benign epithelium to severely atypical epithelium [2].

Mucinous cystadenomas (MCAs) show only mild epithelial dysplasia characterized by a slight increase in the size of nuclei located in lower layers and the absence of mitosis.

Borderline mucinous cystadenomas show moderate dysplasia, characterized by papillary projections or crypts and invaginations with crowding of atypical nuclei and rare mitoses.

Mucinous cystoadenocarcinomas (MCACs) present severe dysplasia/carcinoma in situ which usually occur focally and can only be identified after careful research of multiple sections from different areas of the tumor. The epithelial cells that often form papillae with irregular junctions or arborescence show nuclear stratification, severe nuclear atypia, and frequent mitoses.

MCACs can be further classified into invasive or noninvasive, depending on the presence of stromal invasion. The invasive component usually is similar to the common ductal adenocarcinoma.

5.3.3 MRI

The role of MR Imaging in MCNs includes both the identification and characterization [3, 11].

MCNs appear as oligolocular microcystic or macrocystic lesions, more rarely multilocular, localized in the body-tail (Fig. 5.3). They are rounded in shape and well circumscribed and present a wall with thin internal septa that delimit cystic spaces [5].

On T1-weighted images (performed with fat saturation), the content is homogeneous and hypointense, although the presence of mucin or foci of hemorrhage can increase the intensity of signal.

Because of the fluid content, MCNs are hyperintense on T2-weighted images; the characteristics and the distribution of internal nodularity are well visible in these sequences. The presence of mucin and hemorrhagic foci can make the cyst content inhomogeneous and determines the formation of fluid levels.

Contrast administration makes it easier to recognize the walls, vegetations, or solid components.

Maximum enhancement of wall, mural nodules, and solid components is observed in the venous phase or delayed phase. However, recognition of calcification does not improve after administration of contrast medium.

DWI sequences can facilitate the identification of areas of ADC restriction in correspondence with the solid components of the lesion as the parietal nodules.

The acquisition of images on the coronal plane helps to recognize the characteristics described above.

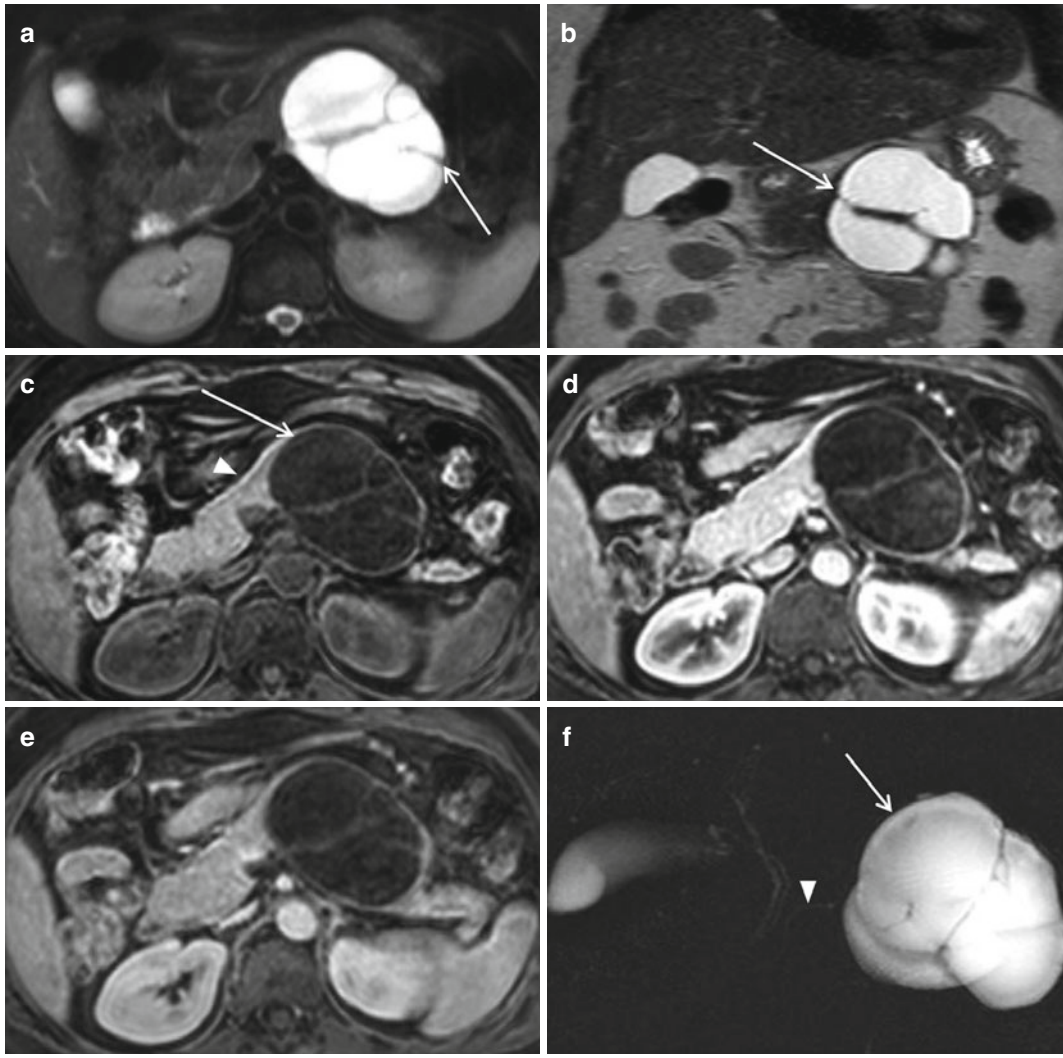

Fig. 5.3 A 76-year-old female patient with mucinous cystadenoma in the body-tail of the pancreas. (**a**, **b**) Axial (**a**) and coronal (**b**) T2-weighted images: a hyperintense cystic mass with septa (*arrow*) is visible. (**c**) Axial T1-weighted GRE image with fat saturation: the content of the lesion (*arrow*) is homogeneously hypointense compared to the adjacent pancreatic parenchyma (*arrow head*). (**d**, **e**) Axial T1-weighted GRE images with fat saturation after contrast administration, in pancreatic (**d**) and portal (**e**) phases: contrast enhancement of walls and septa is visible. (**f**) MRCP image: the cystic lesion is well visible (*arrow*); there is no communication with the main pancreatic duct (*arrowhead*)

The first diagnostic distinction has to be made between mucinous adenomas and adenocarcinomas: adenomas usually present as an oligolocular lesion with septa, while adenocarcinomas tend to have larger size (>4 cm) and a more complex structure.

Cyst walls and septa are typically thicker in adenocarcinomas, which present solid nodules with contrast enhancement.

The content of the cysts in adenomas tends to be more homogeneous, hypointense on T1 images, and hyperintense on T2 images, while fluid inside adenocarcinomas tends to be more heterogeneous and presents a greater hyperintensity on T1 images for the presence of bleeding or solid components. These features are highly suggestive of malignancy of the lesion suggesting surgical resection [14].

In particular, the element which correlates more strongly with the malignancy of MCNs is represented by the presence of parietal nodules.

It can be difficult to differentiate a pseudocyst from a MCN when septa within the lesion are not visible. Otherwise, a positive history of acute or chronic pancreatitis is in favor of pseudocysts [15].

Only a fine-needle aspiration can differentiate with certainty the two cystic lesions: high levels of amylase for pseudocysts and high levels of CEA and CA 19-9 for MCNs.

The classic microcystic form of SCA generally is not a problem for the differential diagnosis, whereas there are rare solid and oligocystic variants of SCA with an appearance that can simulate the MCN. One element that can help in the differential diagnosis between SCAs and MCNs is represented by age, as SCAs tend to occur at a later age than the MCNs.

Branch-duct IPMNs may have a cystic appearance and mimic MCNs. However, the demonstration of communication with the pancreatic ductal system allows to make the differential diagnosis [13, 14]. T2-weighted images (highly sensitive to fluids) are optimal to see the Wirsung duct; the examination can also be completed with MRCP images.

In addition, IPMNs occurred more commonly in men.

5.4 Intraductal Papillary Mucinous Neoplasms

5.4.1 Background

Intraductal papillary mucinous neoplasms (IPMNs) are cystic lesions of the pancreas developing from the mucinous epithelium of the pancreatic ductal system. The cellular atypia is responsible for excessive production of mucin, resulting in dilation of the main pancreatic duct or formation of cystic enlargement of branch ducts.

IPMNs, once considered rare injury, presented in recent years a considerable increase in the incidence, because of technological advancement in diagnostic imaging, currently constituting about 27 % of all cystic neoplasms of the pancreas [11, 16].

Elderly males are mainly affected, with a peak of incidence between 60 and 70 years.

Clinically, nearly half of patients are asymptomatic, and the neoplasm is an incidental finding during an ultrasound examination, CT, or MRI carried out for reasons not correlated to the presence of a cystic pancreatic neoplasm or abdominal pain. Symptoms of IPMNs are nonspecific: in most cases, abdominal pain is present, more rarely jaundice, weight loss, and diabetes.

The role of MR Imaging, currently considered the gold standard in the study of these neoplasms, is to identify the typical signs of IPMNs, to differentiate from other cystic lesions, and to distinguish the various forms of IPMNs, because main-duct IPMNs have a high potential risk of malignancy, significantly greater than branch-duct IPMNs. Therefore, MRI is the first-choice technique to monitor these tumors over time, in order to detect any signs of malignant progression [17].

Main-duct IPMN is characterized by exclusive dilation of the main pancreatic duct, which may be involved in focal or diffuse sense. In most patients with segmental forms, the tumor is located at the body-tail of the pancreas.

Branch-duct IPMNs are characterized by papillary proliferation and mucin hypersecretion within the lumen of the branch ducts. They can present as a single lesion or as multiple cystic lesions (multifocal branch-duct IPMN).

Mixed IPMNs, as the central, predominantly affect male patients (56 % men, 44 % women) and are characterized by the involvement of the main pancreatic duct and one or multiple secondary ducts [11].

5.4.2 Pathology

IPMNs have very wide a spectrum of aggressiveness that depends on the degree of cellular atypia: according to the current WHO classification, they are classified as intraductal papillary mucinous adenoma, borderline IPMN (with moderate dysplasia), and intraductal papillary mucinous carcinoma, noninvasive (in situ) or invasive.

The adenoma is characterized by the presence of columnar epithelium composed of mucin-secreting cells with low-grade atypia. The borderline IPMN is characterized by low degree of dysplasia with epithelial cells that have lost the normal polarity, characterized by the presence of nuclear pyknosis. The intraductal papillary mucinous carcinoma is instead characterized by a high degree of epithelial cell atypia without or with invasion of adjacent tissues (carcinoma in situ and invasive carcinoma, respectively). Within the same tumor, different degrees of dysplasia can be found, suggesting a progressive degeneration from malignant adenoma to borderline tumor, up to carcinoma in situ and finally to invasive carcinoma [2].

The pathologic features suspicious then for dysplastic changes are loss of cell polarity, altered tissue differentiation, high mucin concentration in the cytoplasm, nuclear enlargement, and high rate of mitosis [2].

With regard to immunohistochemical analysis, IPMNs are divided into gastric, intestinal, and biliary neoplasms. The gastric type is primarily associated with branch-duct IPMNs (98 % of cases) and correlates with high-grade dysplasia or invasive carcinoma in only 8 % of cases. The intestinal type, on the contrary, is associated mainly to main-duct IPMNs (73 % of cases) and is correlated to a significantly higher frequency of malignancy (80 %) [57]. Finally, main-duct IPMNs and mixed IPMNs are characterized by a high potential for degeneration with a risk of malignancy of 70 % (57–92 %), while branch-duct IPMNs present a significantly lower risk of degeneration (25 %; average 6–46 %) with a percentage of 15 % developing to invasive carcinoma. In the latter case, the prognosis is comparable to pancreatic adenocarcinoma [18, 19].

5.4.3 MRI

Although computed tomography has a higher spatial resolution, magnetic resonance imaging, in addition to an anatomical representation of the pancreatic parenchyma comparable to CT, presents higher contrast resolution and with MRCP images allows the representation of the ductal system [20].

On T1-weighted images, IPMNs appear as single or multiple ductal dilations, homogeneously hypointense compared with the surrounding pancreatic parenchyma (Fig. 5.4). Hypointensity is more evident in the sequences performed with fat saturation due to the higher signal from the adjacent pancreatic parenchyma. On T2-weighted images, the content of the cyst fluid is markedly hyperintense compared to the surrounding parenchyma. A more accurate evaluation is possible with MRCP images which allow to obtain an anatomical representation of pancreatic-biliary ductal system. MRCP images can evaluate the localization and extension of the cystic lesion, the presence of dilated side branches, or intraluminal filling defects.

Finally, the dynamic phase after administration of contrast medium is essential for the assessment of signs of degeneration. Mural nodules closely adherent to the cystic part of the tumor are associated with malignant degeneration. The greatest difficulty is to identify these nodules when they are still small in size, in order to make an early diagnosis of IPMN with aggressive potential. Another radiological sign predictive of malignancy is the contrast enhancement of the IPMN walls [10, 17, 21].

Main-duct IPMNs appear as focal or diffuse dilation of the main pancreatic duct (Fig. 5.5). They generally have a fusiform appearance and walls consisting of ductal epithelium. In focal forms, the involvement of the body-tail is characterized by the presence of localized dilation in the distal part of the pancreas, leaving the parenchyma of the head unscathed; on the contrary, the involvement of the pancreatic head is often accompanied by dilation of the entire upstream duct. The localization of the dilation of the main pancreatic duct is not related to the biological behavior of the tumor [17].

Main-duct IPMNs enter into the differential diagnosis mainly with different causes of ductal dilation. In particular, in the presence of diffuse forms of main-duct IPMN, the pancreas may be very similar to a picture of chronic obstructive pancreatitis. The presence of mucin deposits

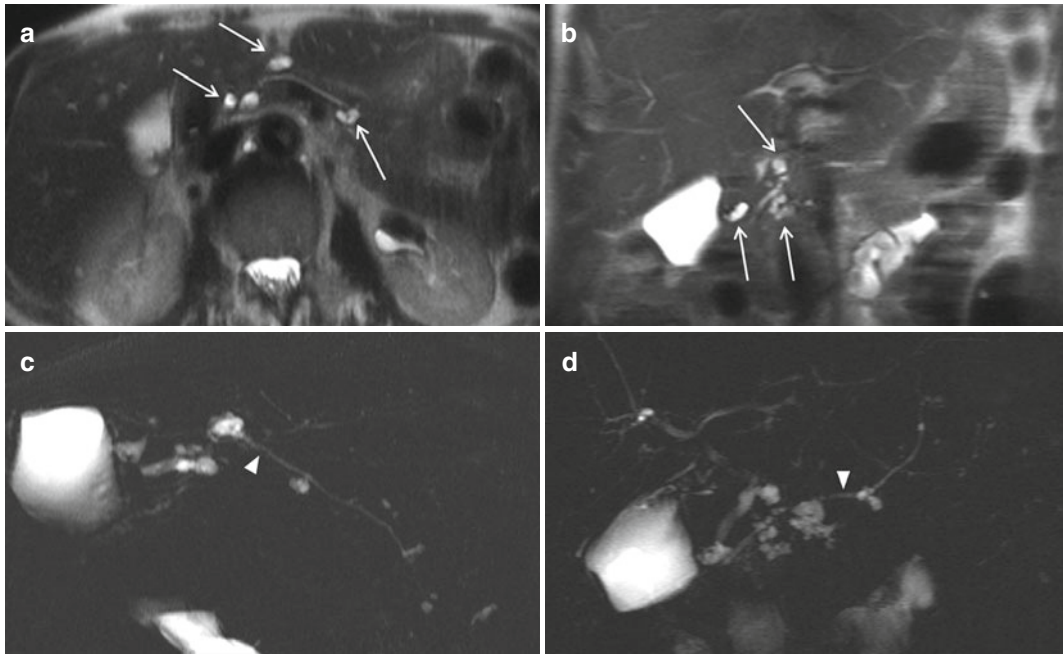

Fig. 5.4 A 57-year-old female patient with multifocal branch-duct IPMNs. (**a**, **b**) Axial (**a**) and coronal (**b**) T2-weighted images: multiple cystic dilations of pancreatic branch ducts (*arrows*) are visible along the whole gland, hyperintense compared to the surrounding parenchyma. (**c**, **d**) Axial (**c**) and coronal (**d**) MRCP images: IPMNs are depicted in pancreatic head, body, and tail; the connection with the main pancreatic duct (*arrowhead*) is well visible for all the cysts

within the cyst is characteristic of IPMNs. These deposits appear as filling defects mildly hyperintense on T1-weighted images and markedly hypointense on T2 images compared to the fluid content of the lesion; on the contrary, the presence of diffuse calcifications is associated mainly with the presence of chronic pancreatitis.

Mixed IPMNs are characterized by the presence of diffuse dilation of the main pancreatic duct and one or multiple dilated side ducts (Fig. 5.5).

Side-branch IPMNs appear as single or multiple cystic lesions, round or oval, communicating with the lumen of the main pancreatic duct, which presents normal caliber.

Imaging appearance of branch-duct IPMNs may be similar to other cystic neoplasms, such as mucinous cystic neoplasms (MCNs). While MCNs preferentially affect women (95 % of cases) with an age range between 40 and 50 and are located in most of the cases in the body-tail, IPMNs primarily affect elder male patients; Furthermore, the presence of multiple cystic dilations throughout the pancreatic parenchyma is more indicative of IPMN [21].

The definitive diagnosis of branch-duct IPMN occurs, however, with the demonstration of communication between the cystic lesion and the main pancreatic duct. MRCP images are the best for the evaluation of such communication.

In the past, several studies have been conducted on the use of pharmacological stimulation with secretin for a better view of the ductal system, but in almost all cases, the communication with the main pancreatic duct can be depicted on MCRP images in basal conditions, without the need of secretin stimulation [14, 22].

Another important role of diagnostic imaging is to monitor over time these tumors in order to identify early signs suggestive of malignant degeneration.

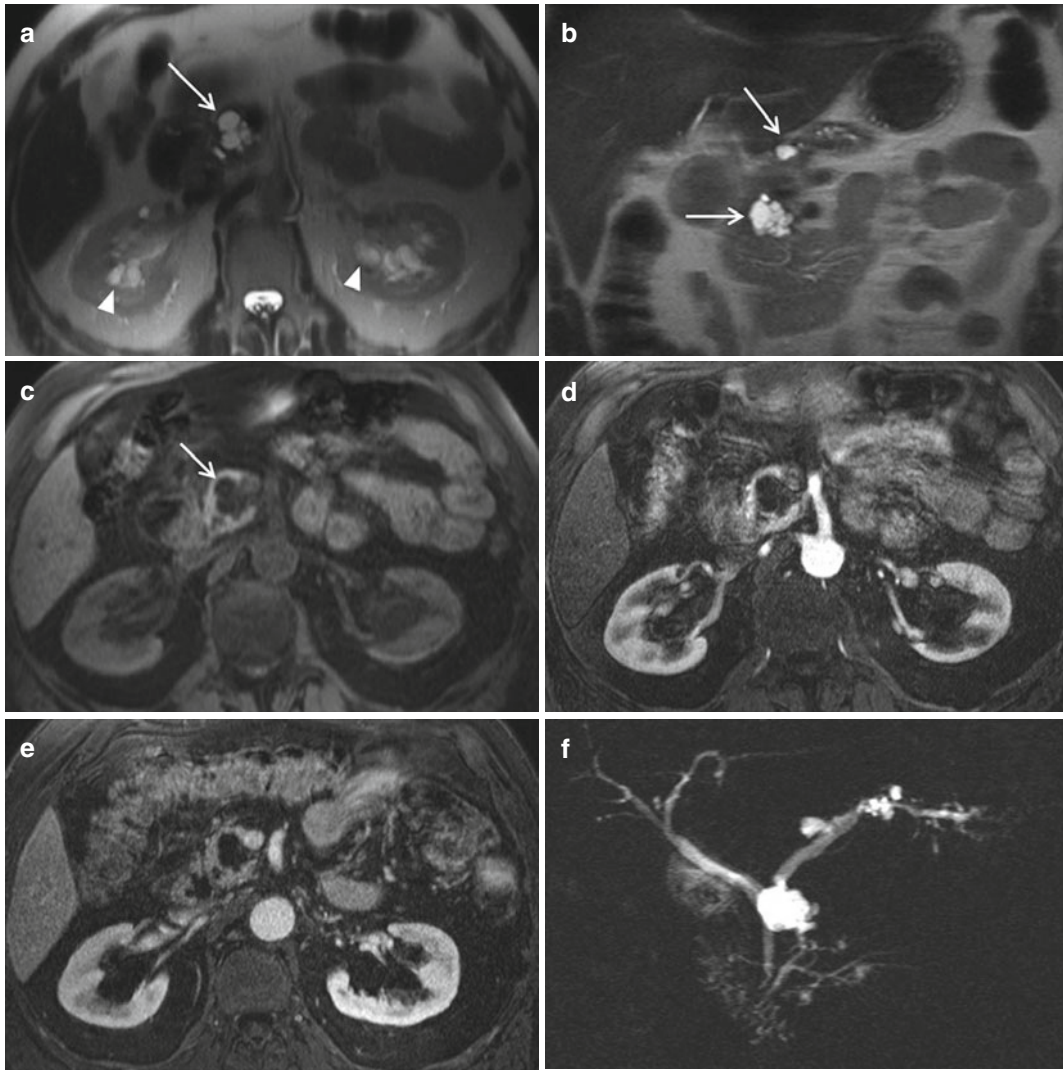

Fig. 5.5 A 57-year-old female patient with multifocal branch-duct IPMNs and main-duct IPMN (mixed IPMN). (**a**, **b**) Axial (**a**) and coronal (**b**) T2-weighted images: multiple cystic dilations of pancreatic branch ducts (*arrows*) are visible along the whole gland, hyperintense compared to the surrounding parenchyma; main pancreatic duct is dilated, too; note the presence of multiple cysts in the kidneys (*arrowheads*). (**c**) Axial T1-weighted GRE image with fat saturation: IPMNs (*arrow*) appear hypointense compared to the surrounding pancreatic parenchyma. (**d**, **e**) Axial T1-weighted GRE images with fat saturation after contrast administration, in pancreatic (**d**) and portal (**e**) phases: there are no mural nodules within cystic lesions. (**f**) MRCP image: IPMNs are depicted in pancreatic head, body, and tail; the connection with the main pancreatic duct, greatly dilated, is well visible for all the cysts

The signs that better correlate with the degeneration are (1) the presence of cystic lesions >3 cm in diameter, (2) the presence of vegetations or mural nodules >3 mm in diameter, (3) contrast enhancement of the walls of the pancreatic duct involved, and (4) dilation of the main pancreatic duct >18 mm.

5.5 Solid Pseudopapillary Neoplasms

5.5.1 Background

Solid pseudopapillary neoplasms (SPNs) of the pancreas are rare lesions with a frequency

between 0.9 and 2.7 % of all pancreatic tumors and 4 % of cystic neoplasms [23, 24].

SPN was described for the first time in 1959 by Franz and characterized by Haimoudi in 1970. Only in 1996, the World Health Organization has reclassified according to its pathologic features this solid-cystic neoplasm giving it the name of "solid pseudopapillary tumor" of the pancreas and renamed in 2010 "solid pseudopapillary neoplasm," name accepted and internationally recognized [23].

SPN preferentially affects young women (incidence peak between 20 and 30 years), with a male to female ratio of 1:9 [24].

The pathogenesis of this tumor remains unknown; some authors have suggested the association with pregnancy or polycystic ovaries. The prevalence in females during puberty has in the past suggested the existence of a relationship between tumor growth and female sex hormones [25, 26].

The lesions can be localized in any region of the gland, and the diagnosis usually occurs in discrete sizes: 8–10 cm in average with a range between 0.5 and 25 cm [26]. The tumor size at diagnosis does not correlate directly with increased malignancy or with a worse prognosis. There is no clinical evidence of a correlation between the tumor occurrence and some extrinsic factors such as alcohol, coffee, and cigarette smoke [24].

Although it can usually remain asymptomatic, due to its considerable size, SPN can determine clinical symptoms of stomach compression such as nausea, fullness, or dull epigastric pain [27]. Rarely weight loss, dyspepsia, and jaundice can also be observed, and occasionally lesions are identified directly on physical examination as palpable masses. In some cases, the disease is diagnosed incidentally during the execution of clinical and instrumental examinations performed for other reasons. Laboratory data are not diagnostic; these tumors do not seem to be associated with any marker in use [23].

At diagnosis most SPNs are localized only in the pancreatic gland without infiltration of the surrounding structures, characterizing it as a benign neoplasm. In 5–15 % of patients, however, liver metastases are present at diagnosis; but even in these cases, the low degree of aggressiveness of SPN determines a good prognosis [25]. The 5-year survival rate is currently over 90 % in all those patients who have undergone a radical tumor resection [25].

5.5.2 Pathology

SPN usually manifests as a solitary intrapancreatic mass. Rare is the infiltration of adjacent structures; at diagnosis usually SPNs present with considerable size. Macroscopically, the neoplasm appears as a round or oval well-circumscribed lesion with sharp margins, separated from the surrounding healthy pancreas by a fibrous capsule [28]. Sometimes calcification and septa can be found within the lesion although these are not diagnostic [23]. The tissue inside the neoplasm is usually more or less parenchymatous with presence of cystic areas due to necrotic-bleeding phenomena.

SPN in fact origins a solid mass, and only after months/years its increase in volume, poorly supported by an adequate blood supply, causes a gradual loss of neoplastic tissue with consequent formation of pseudopapillae, necrosis, and bleeding [29, 30]. The alternation of solid and cystic areas results in the pathognomonic aspect of the lesion, even if the relationship between the two components is very variable. Histologically two main types of cells are found: in the solid areas, a layer of neoplastic cells, and in the pseudopapillary component, a fibrovascular axis, surrounded by one or two layers of columnar epithelium [31].

5.5.3 MRI

SPN of the pancreas is a rare expansive lesion that can occur at any site of the pancreatic parenchyma, with sizes ranging from small to very big. The lesion is generally round or oval, with sharp edges and a thin wall; in smaller lesions, the wall may be difficult to appreciate [23, 29, 31] (Fig. 5.6).

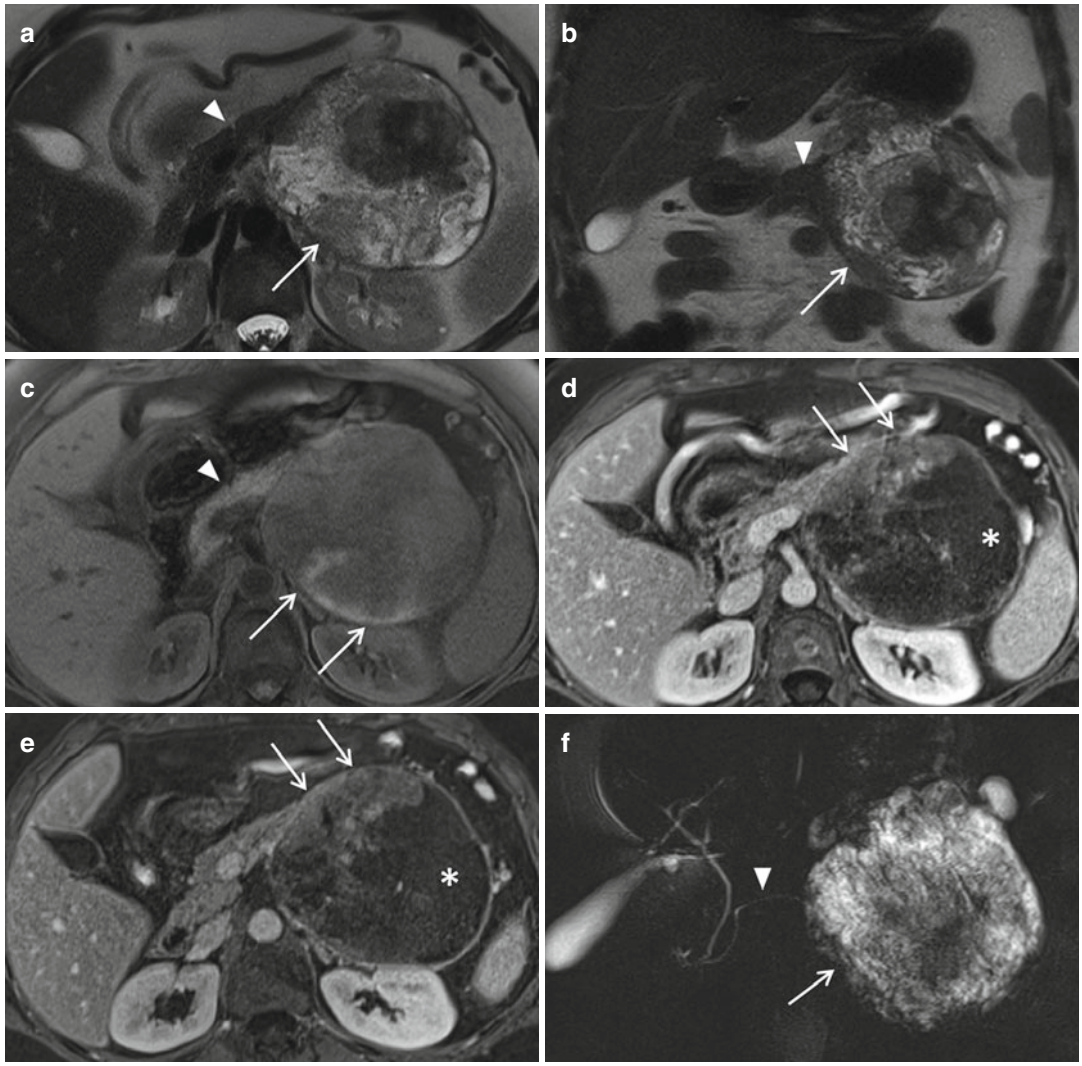

Fig. 5.6 A 43-year-old female patient with solid pseudopapillary neoplasm (SPN). (**a**, **b**) Axial (**a**) and coronal (**b**) T2-weighted images: a cystic lesion (*arrow*) is present in the tail of the pancreas; it is heterogeneously hyperintense compared to the surrounding pancreatic parenchyma (*arrowhead*). (**c**) Axial T1-weighted GRE image with fat saturation: the neoplasm is hypointense compared to the surrounding pancreatic parenchyma (*arrowhead*); hyperintense areas correspond to intralesional hemorrhage (*arrows*). (**d**, **e**) Axial T1-weighted GRE images with fat saturation after contrast administration, in pancreatic (**d**) and portal (**e**) phases: the capsule and the solid portion of the lesion (*arrow*) show contrast enhancement; cystic and hemorrhagic regions appear hypointense (*asterisk*). (**f**) MRCP image: the large cystic component of the mass (*arrow*) presents an intermediate signal in relation to the hemorrhagic intralesional component; main pancreatic duct is not dilated (*arrowhead*)

The mass is hypointense on T1-weighted images and heterogeneously hyperintense on T2-weighted images compared to the surrounding healthy pancreatic parenchyma; its signal is homogeneous or heterogeneous in relation to the different percentage of solid and cystic/hemorrhagic components [23, 24]. MRI is therefore the most effective technique to identify the presence of intralesional blood; the hemorrhagic areas present a signal variability related to the hemoglobin degradation [28]. The presence of an intralesional hyperintense zone on T1-weighted fat-suppressed images with low signal on T2 images indicates the presence of various metabolites of hemoglobin, such as methemoglobin and hemosiderin [32]. Note the appearance of these necrotic-hemorrhagic

portions is usually uneven and sometimes fluid levels can also be observed [24, 28]. In addition to these aspects, it is necessary to remember that in large tumors there is a significant presence of cystic component, which appears hypointense on T1 images and markedly hyperintense on T2 images. In these images, it is easy to recognize the thick wall and the solid portion of the neoplasm represented by pseudopapillae [23, 29].

The fibrous capsule on T1-weighted images is hardly distinguishable from the lesion because of the small size and the hypointense signal; it presents low signal intensity on T2-weighted images, separating the lesion from the healthy adjacent pancreatic parenchyma [23, 29]. After contrast injection, the wall and the solid components present contrast enhancement. Solid areas, better identified after contrast administration, are noticed mainly at the periphery, while the cystic components are located most frequently in the center of the lesion [5, 23, 29].

The internal solid and cystic architecture is clearly visible both on MRI and CT images, but bleeding is more clearly delineated on MRI [29]. The presence of calcification instead represents a rare occurrence; in this case, CT is the first-line investigation.

Only rare cases of liver metastases from SPN of the pancreas have been described; even more rarely involvement and dilation of the main pancreatic duct upstream the lesion with pancreatic parenchyma atrophy have been observed. These features together with the presence of a fibrous capsule and hemorrhagic areas are key elements to differentiate SPNs from other cystic lesions of the pancreas [23, 29, 31].

When this neoplasm has an important cystic component, it can be confused with a mucinous cystic neoplasm. The latter, however, is localized preferentially in the body-tail, and it may be responsible for compressive phenomena, with dilation of the main pancreatic duct.

Serous cystadenoma compared to SPN is more frequently polycystic and microcystic; its margins are lobulated and contrast enhancement of the septa within the lesion can be observed. The presence of a central fibrous scar, not typical of SPN, with or without calcifications, indicates the presence of serous cystadenoma [5].

At diagnosis nonfunctioning neuroendocrine tumors can grow to considerable size, with consequent increase in the incidence of calcification, cystic degeneration, or central areas of necrosis and hemorrhage. However, their marked hypervascularity during the arterial phase of the dynamic study is useful for the differential diagnosis [23, 29].

Mucinous cystic neoplasms, serous cystadenoma, and neuroendocrine tumors are lesions that must always be considered in the differential diagnosis with solid pseudopapillary neoplasm in the presence of a cystic/solid pancreatic mass [3, 15].

5.6 Neuroendocrine Tumors

5.6.1 Background

Pancreatic neuroendocrine tumors (NETs) are rare tumors, 2–10 % of all primary tumors of the pancreas. They originate from multipotent stem cells of the ductal epithelium and show endocrine differentiation.

The mortality rate is significantly lower compared to pancreatic adenocarcinoma with a median survival of 7.1 years after complete resection; survival is reduced to 5.2 in cases of locally advanced disease without metastases and 2.1 years in presence of metastases.

Pancreatic NETs have no predilection for age or sex and are located in any portion of the pancreas; preferential locations depend on the histological type [33].

In 10–30 % of cases, NETs are found in patients with hereditary syndromes: MEN (multiple endocrine neoplasia) or von Hippel-Lindau syndrome (VHL).

Clinically NETs are classified as "functioning" and "nonfunctioning" tumors, in relation to the presence or absence of a specific clinical syndrome induced by hormone secretion.

Nonfunctioning NETs are the most common (60–80 % of all NETs); insulinomas and gastrinomas are the most common functioning NETs.

Clinically, these two types of cancer occur in very different ways: functioning NETs show the effects of increase hormone secretion; nonfunctioning NETs present symptoms related to

compression or to the presence of metastases. In MEN-1 patients (characterized by pituitary adenomas, endocrine tumors, and hyperparathyroidism), pancreatic NETs are found in 40–80 % of patients, mainly nonfunctioning NETs. Multiple pancreatic NETs are found in 10–15 % of patients with von Hippel-Lindau syndrome [34].

Although NETs tend to be less aggressive than adenocarcinoma, they often metastasize to the liver. At diagnosis, except for insulinomas, 50–60 % of NETs present liver metastases.

5.6.2 Pathology

According the World Health Organization (WHO) classification, pancreatic NETs are divided in well-differentiated and poorly differentiated tumors.

Well-differentiated NETs have the characteristic "organoid" aspect of tumor cells, with trabecular features. Cells are generally uniform and produce abundant neurosecretory granules, reflecting the marked and diffuse immunoexpression of neuroendocrine markers such as A chromogranin A and synaptophysin.

Poorly differentiated NETs have a chaotic architecture, with irregular nuclei and poor cytoplasmic granularity. The immunoexpression of neuroendocrine markers is typically limited.

In 2006 the European Neuroendocrine Tumor Society (ENETS) proposed a classification based on the expression of mitotic index Ki67. The classification was adopted and extended by WHO in 2010:

- G1: $\leq$ 2 mitoses per 2 mm^2 and Ki-67 index $\leq 2\%$
- G2: = 2–20 mitoses per 2 mm^2 or Ki-67 index between 3 and 20 %
- G3: $\geq$ 21 mitoses per 2 mm^2 or Ki-67 index $> 20\%$

G1 and G2 (low and intermediate grades) correspond to well-differentiated NETs and show the expression of chromogranin A and synaptophysin; G3 (high grade) indicates a poorly differentiated tumor (endocrine carcinoma) [34].

The 5-year survival rate for nonfunctioning well-differentiated NET is between 60 and 100 %; for poorly differentiated carcinomas it is 29 %.

Generally pancreatic NETs occur as solid rounded single lesions, with or without a capsule. Their dimensions are 0.5–1 cm for insulinomas and up to 10 cm for nonfunctioning NETs.

In rare cases, these masses appear considerably hemorrhagic, with bluish-purple color and soft texture. Sometimes fibrosis is massive and gives hard consistency and a whitish color.

Necrotic foci can be found within the lesions, especially in malignant masses; necrosis, if abundant, gives a cystic aspect to the neoplasm. In these cases, the differential diagnosis with cystic tumor or pseudopapillary neoplasm can be difficult.

NETs can sometimes show aspects of malignant tumors: irregular margins; infiltration of perivisceral adipose tissue, mainly through satellite nodules; and infiltration of the duodenal wall, common bile duct, spleen, or vessels. The involvement of splenic vessels with vascular thrombosis can cause splenic infarcts.

The cytological examination of material obtained by FNAB (fine-needle biopsy) is the most widely used technique for the diagnosis of pancreatic masses.

In most cases, the histological appearance of the tumors is sufficient to suggest the endocrine origin.

The presence of amyloid extracellular deposits is frequently observed in insulinomas. Because these tumors usually grow slowly, the normal structures such as ducts and pancreatic islets can be trapped inside the tumor.

5.6.3 MRI

Magnetic resonance imaging (MRI) is frequently used for the identification of pancreatic NETs and it is complementary to CT; MRI can be used to confirm a CT finding or to locate a suspicious lesion not depicted at CT. MRI advantages are the high contrast resolution, the high sensitivity

of dynamic study, and the optimal visualization of pancreatic ductal system.

Nowadays MRI devices allow rapid breath-hold acquisitions, even after contrast administration, with significant reduction of motion artifacts. Diffusion-weighted imaging (DWI) is helpful for the identification of small pancreatic NETs. During the same examination, the liver can also be examined, and MRI presents higher accuracy to depict liver metastases compared to CT [35, 36].

NETs generally have hypointense signal on T1-weighted images with fat suppression and hyperintense signal on T2-weighted images compared to surrounding pancreatic tissue [37].

After contrast administration, there is a typical marked and homogeneous contrast enhancement of the lesion in both pancreatic and portal phases, which reflects the high vascularization of the tumor; in cystic NETs, there is contrast enhancement of the peripheral rim (Fig. 5.7).

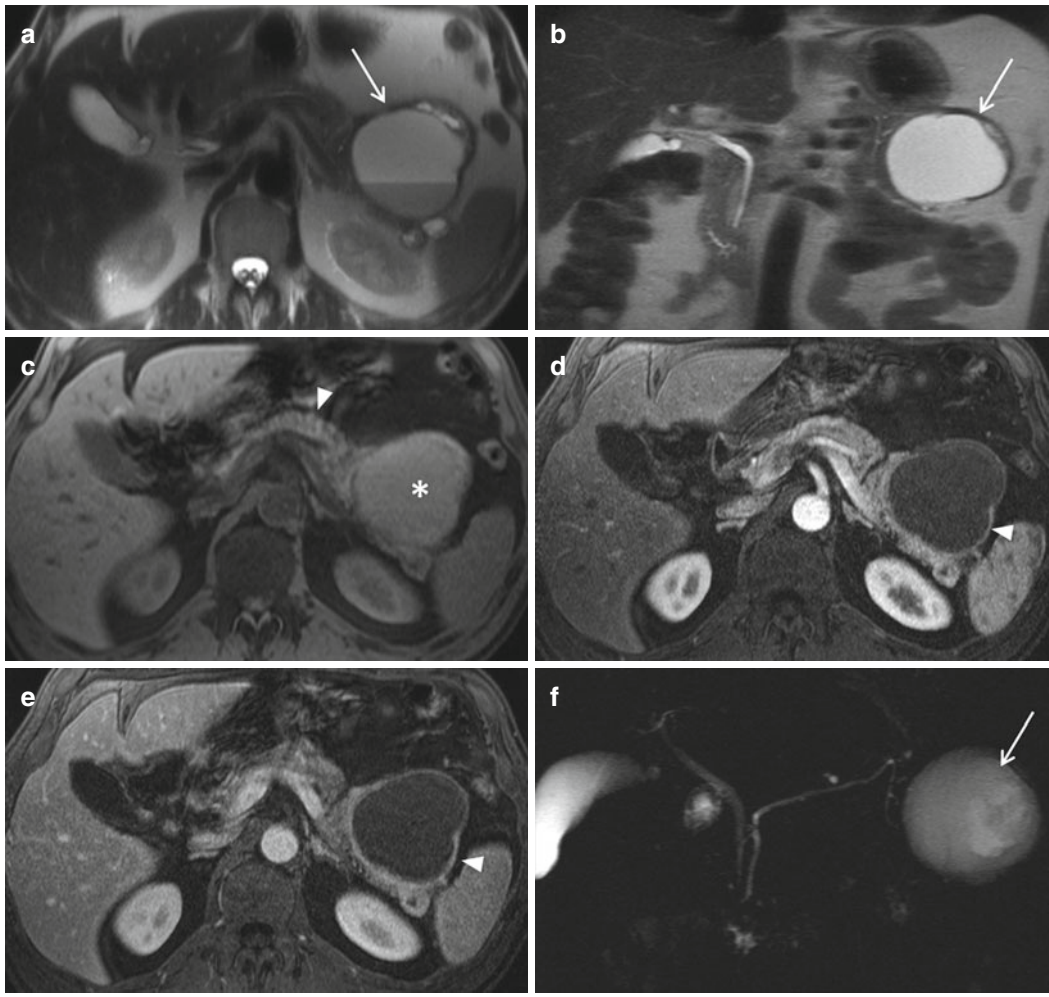

Fig. 5.7 A 58-year-old patient with cystic pancreatic neuroendocrine tumor. (**a**, **b**) Axial (**a**) and coronal (**b**) T2-weighted images: a hyperintense cystic mass (*arrow*) is visible in the pancreatic tail; intracystic fluid contains blood and presents two different signal intensities, because of the presence of different hemoglobin metabolites. (**c**) Axial T1-weighted GRE image with fat saturation: intracystic fluid (*asterisk*) is isointense to pancreatic parenchyma (*arrowhead*) because of the presence of blood inside the cyst. (**d**, **e**) Axial T1-weighted GRE images with fat saturation after contrast administration, in pancreatic (**d**) and portal (**e**) phases: cystic walls are hypervascularized (*arrowhead*). (**f**) MRCP image: cystic lesion is hyperintense (*arrow*) and it does not communicate with the main pancreatic duct

Larger tumors show a more heterogeneous contrast enhancement.

At DWI sequences, NETs usually present hyperintense signal at high-b-value images and hypointensity on ADC maps, with ADC values significantly lower than healthy pancreas [8, 9]. ADC value may vary according to specific histopathological features, such as the differentiation degree, the coexistence of intralesional hemorrhage, necrosis, and the cellularity degree. Some studies show that apparent diffusion coefficient (ADC) correlates with Ki-67 value, showing a decrease in ADC value in tumors with high expression of Ki-67 [38].

NET metastatic lesions reflect the characteristics of the primary tumor. Their most common site is the liver. Liver metastases generally are hypointense on T1-weighted images and hyperintense on T2-weighted images. In the dynamic study after contrast administration, metastatic lesions are hyperintense in the arterial phase and relatively hypointense in the portal venous phase.

In approximately 5% of cases, pancreatic NETs present as cystic lesions (Fig. 5.7), and this aspect is found more frequently in MEN-1 patients. Cystic degeneration can also occur, mainly in functioning NET [39].

There are two forms of cystic NETs:

- Macrocystic form, characterized by the presence of a limited number (<3) of cysts with islands of neuroendocrine cells within the wall: these forms are very similar to mucinous cystic neoplasms.
- Microcystic form, characterized by the presence of numerous small cavitations localized within the tumor mass and surrounded by tumor cells; these forms are very similar to serous cystadenomas.

The preoperative diagnosis can be difficult because, although often these tumors secrete glucagon, sometimes they are nonfunctioning.

The fluid inside the cysts is hypointense on T1-weighted images and hyperintense on T2-weighted images; the wall thickness is variable. The appearance is identical to other cystic lesions of the pancreas, and often a definitive diagnosis can be obtained only after histological examination. The wall sometimes is calcified and presents early contrast enhancement in the arterial phase.

The prognosis of cystic forms is better than solid pancreatic NETs [40]. The presence of calcifications and the lack of ductal stenosis and vascular invasion can be useful aspects to differentiate NETs from adenocarcinomas.

References

1. Adet A, Miquel R, Bombi JA, Gines A, Fernandez-Esparrach G, De Juan C, et al. Incidence and characteristics of pancreatic cystic neoplasms. Gastroenterol Hepatol. 2010;33(8):563–8.
2. Zamboni G, Scarpa A, Bogina G, Iacono C, Bassi C, Talamini G, et al. Mucinous cystic tumors of the pancreas: clinicopathological features, prognosis, and relationship to other mucinous cystic tumors. Am J Surg Pathol. 1999;23(4):410–22.
3. Morana G, Guarise A. Cystic tumors of the pancreas. Cancer Imaging Off Publ Int Cancer Imaging Soc. 2006;6:60–71.
4. Salvia R, Crippa S, Falconi M, Bassi C, Guarise A, Scarpa A, et al. Branch-duct intraductal papillary mucinous neoplasms of the pancreas: to operate or not to operate? Gut. 2007;56(8):1086–90.
5. Kalb B, Sarmiento JM, Kooby DA, Adsay NV, Martin DR. MR imaging of cystic lesions of the pancreas. Radiographics Rev Publ Radiol Soc North Am Inc. 2009;29(6):1749–65.
6. Sakorafas GH, Smyrniotis V, Reid-Lombardo KM, Sarr MG. Primary pancreatic cystic neoplasms revisited. Part I: serous cystic neoplasms. Surg Oncol. 2011;20(2):e84–92.
7. Tseng JF. Management of serous cystadenoma of the pancreas. J Gastrointest Sur Off J Soc Surg Aliment Tract. 2008;12(3):408–10.
8. Bassi C, Salvia R, Gumbs AA, Butturini G, Falconi M, Pederzoli P. The value of standard serum tumor markers in differentiating mucinous from serous cystic tumors of the pancreas: CEA, Ca 19-9, Ca 125, Ca 15-3. Langenbeck's Arch Surg/Deutsche Gesellschaft fur Chirurgie. 2002;387(7-8):281–5.
9. Boraschi P, Donati F, Gigoni R, Salemi S, Bartolozzi C, Falaschi F. Diffusion-weighted MRI in the characterization of cystic pancreatic lesions: usefulness of ADC values. Magn Reson Imaging. 2010;28(10):1447–55.
10. Guarise A, Faccioli N, Ferrari M, Salvia R, Mucelli RP, Morana G, et al. Evaluation of serial changes of pancreatic branch duct intraductal papillary mucinous neoplasms by follow-up with magnetic resonance imaging. Cancer Imaging. 2008;8:220–8.

11. Kosmahl M, Pauser U, Peters K, Sipos B, Luttges J, Kremer B, et al. Cystic neoplasms of the pancreas and tumor-like lesions with cystic features: a review of 418 cases and a classification proposal. Virchows Archiv Int J Pathol. 2004;445(2):168–78.
12. Zamboni G, Bonetti F, Scarpa A, Pelosi G, Doglioni C, Iannucci A, et al. Expression of progesterone receptors in solid-cystic tumour of the pancreas: a clinicopathological and immunohistochemical study of ten cases. Virchows Arch A Pathol Anat Histopathol. 1993;423(6):425–31.
13. Procacci C, Graziani R, Bicego E, Zicari M, Bergamo Andreis IA, Zamboni G, et al. Papillary cystic neoplasm of the pancreas: radiological findings. Abdom Imaging. 1996;21(3):554–8.
14. Manfredi R, Bonatti M, D'Onofrio M, Mehrabi S, Salvia R, Mantovani W, et al. Incidentally discovered benign pancreatic cystic neoplasms not communicating with the ductal system: MR/MRCP imaging appearance and evolution. Radiol Med. 2013;118(2):163–80.
15. Kim YH, Saini S, Sahani D, Hahn PF, Mueller PR, Auh YH. Imaging diagnosis of cystic pancreatic lesions: pseudocyst versus nonpseudocyst. Radiographics Rev Publ Radiol Soc North Am Inc. 2005;25(3):671–85.
16. Tanaka M, Chari S, Adsay V, Fernandez-del Castillo C, Falconi M, Shimizu M, et al. International consensus guidelines for management of intraductal papillary mucinous neoplasms and mucinous cystic neoplasms of the pancreas. Pancreatology Off J Int Assoc Pancreatol. 2006;6(1-2):17–32.
17. Manfredi R, Graziani R, Motton M, Mantovani W, Baltieri S, Tognolini A, et al. Main pancreatic duct intraductal papillary mucinous neoplasms: accuracy of MR imaging in differentiation between benign and malignant tumors compared with histopathologic analysis. Radiology. 2009;253(1):106–15.
18. Salvia R, Crippa S, Partelli S, Armatura G, Malleo G, Paini M, et al. Differences between main-duct and branch-duct intraductal papillary mucinous neoplasms of the pancreas. World J Gastrointest Surg. 2010;2(10):342–6.
19. Vullierme MP, d'Assignies G, Ruszniewski P, Vilgrain V. Imaging IPMN: take home messages and news. Clin Res Hepatol Gastroenterol. 2011;35(6-7):426–9.
20. Irie H, Honda H, Aibe H, Kuroiwa T, Yoshimitsu K, Shinozaki K, et al. MR cholangiopancreatographic differentiation of benign and malignant intraductal mucin-producing tumors of the pancreas. AJR Am J Roentgenol. 2000;174(5):1403–8.
21. Manfredi R, Mehrabi S, Motton M, Graziani R, Ferrari M, Salvia R, et al. MR imaging and MR cholangiopancreatography of multifocal intraductal papillary mucinous neoplasms of the side branches: MR pattern and its evolution. Radiol Med. 2008;113(3):414–28.
22. Carbognin G, Pinali L, Girardi V, Casarin A, Mansueto G, Mucelli RP. Collateral branches IPMTs: secretin-enhanced MRCP. Abdom Imaging. 2007;32(3):374–80.
23. Ventriglia A, Manfredi R, Mehrabi S, Boninsegna E, Negrelli R, Pedrinolla B, et al. MRI features of solid pseudopapillary neoplasm of the pancreas. Abdom Imaging. 2014.
24. Sun CD, Lee WJ, Choi JS, Oh JT, Choi SH. Solid-pseudopapillary tumours of the pancreas: 14 years experience. ANZ J Surg. 2005;75(8):684–9.
25. Coleman KM, Doherty MC, Bigler SA. Solid-pseudopapillary tumor of the pancreas. Radiographics Rev Publ Radiol Soc North Am Inc. 2003;23(6):1644–8.
26. Cooper JA. Solid pseudopapillary tumor of the pancreas. Radiographics Rev Publ Radiol Soc North Am Inc. 2006;26(4):1210.
27. Hav M, Lem D, Chhut SV, Kong R, Pauwels P, Cuvelier C, et al. Clear-cell variant of solid-pseudopapillary neoplasm of the pancreas: a case report and review of the literature. Malays J Pathol. 2009;31(2):137–41.
28. Papavramidis T, Papavramidis S. Solid pseudopapillary tumors of the pancreas: review of 718 patients reported in English literature. J Am Coll Surg. 2005;200(6):965–72.
29. Yu MH, Lee JY, Kim MA, Kim SH, Lee JM, Han JK, et al. MR imaging features of small solid pseudopapillary tumors: retrospective differentiation from other small solid pancreatic tumors. AJR Am J Roentgenol. 2010;195(6):1324–32.
30. Zhang H, Liang TB, Wang WL, Shen Y, Ren GP, Zheng SS. Diagnosis and treatment of solid-pseudopapillary tumor of the pancreas. Hepatobiliary Pancreat Dis Int HBPD INT. 2006;5(3):454–8.
31. Yao X, Ji Y, Zeng M, Rao S, Yang B. Solid pseudopapillary tumor of the pancreas: cross-sectional imaging and pathologic correlation. Pancreas. 2010;39(4):486–91.
32. Choi JY, Kim MJ, Kim JH, Kim SH, Lim JS, Oh YT, et al. Solid pseudopapillary tumor of the pancreas: typical and atypical manifestations. AJR Am J Roentgenol. 2006;187(2):W178–86.
33. Ehehalt F, Saeger HD, Schmidt CM, Grutzmann R. Neuroendocrine tumors of the pancreas. Oncologist. 2009;14(5):456–67.
34. Klimstra DS, Modlin IR, Coppola D, Lloyd RV, Suster S. The pathologic classification of neuroendocrine tumors: a review of nomenclature, grading, and staging systems. Pancreas. 2010;39(6):707–12.
35. Rockall AG, Reznek RH. Imaging of neuroendocrine tumours (CT/MR/US). Best Pract Res Clin Endocrinol Metab. 2007;21(1):43–68.
36. Hayashi D, Tkacz JN, Hammond S, Devenney-Cakir BC, Zaim S, Bouzegaou N, et al. Gastroenteropancreatic neuroendocrine tumors: multimodality imaging features with pathological correlation. Jpn J Radiol. 2011;29(2):85–91.
37. Chang S, Choi D, Lee SJ, Lee WJ, Park MH, Kim SW, et al. Neuroendocrine neoplasms of the gastrointestinal tract: classification, pathologic basis, and imaging features. Radiographics Rev Publ Radiol Soc North Am Inc. 2007;27(6):1667–79.

38. Schmid-Tannwald C, Schmid-Tannwald CM, Morelli JN, Neumann R, Haug AR, Jansen N, et al. Comparison of abdominal MRI with diffusion-weighted imaging to 68Ga-DOTATATE PET/CT in detection of neuroendocrine tumors of the pancreas. Eur J Nucl Med Mol Imaging. 2013;40(6):897–907.
39. Kadota Y, Shinoda M, Tanabe M, Tsujikawa H, Ueno A, Masugi Y, et al. Concomitant pancreatic endocrine neoplasm and intraductal papillary mucinous neoplasm: a case report and literature review. World J Surg Oncol. 2013;11:75.
40. Scoazec JY, Vullierme MP, Barthet M, Gonzalez JM, Sauvanet A. Cystic and ductal tumors of the pancreas: diagnosis and management. J Visc Surg. 2013;150(2):69–84.